JOURNAL OF MATERIALS SCIENCE 13 (1978) 2013–2021

Activated slip systems during yielding of α-β brass two-phase bicrystals

TAKAYUKI TAKASUGI, OSAMU IZUMI
The Research Institute for Iron, Steel and Other Metals, Tohoku University, Sendai, Japan

NABIL FAT-HALLA*
Graduate School, Tohoku University, Sendai, Japan

α–β brass two-phase bicrystals, consisting of f c c (α) single crystals and b c c (β) single crystals, which were made by the solid state diffusion couple technique, were tensile-tested at room temperature in order to clarify the role of phase-interface on the deformation. The two-phase bicrystals had small concentration gradients in the α- and β-phases and satisfied the Kurjumov–Sach's orientation relationships i.e. $\{1\,1\,1\}_\alpha \parallel \{1\,1\,0\}_\beta$ and $[1\,1\,0]_\alpha \parallel [1\,1\,1]_\beta$ at the interface. The slip traces observed in bicrystals deformed to about 3% plastic strain showed a striking contrast between the α- and β-phases; the slip traces in the α-phase were clear and straight, while those in the β-phase were fine and wavy. The slip systems in the bicrystals were attributed to those observed in α and β single crystals, and were explained by a plastic strain incompatibility mechanism. The slip systems, originating at the interface or propagating from another phase, were observed on matching planes.

1. Introduction

Mechanical characteristics of mono- and two-phase polycrystals depend on not only the properties of constituent phase, but also on the roles of grain boundaries and phase-interfaces. The role of grain boundaries on deformation of mono-phase polycrystals has been clarified by using the bicrystals composed of f c c [1–3], b c c [4–8] and h c p [9, 10] lattices. From such research some basic factors controlling the deformation of polycrystals have been discovered; one is the elastic compatibility effect and another is the plastic compatibility effect.

However, there has been little fundamental research carried out concerning the effect of phase-interface on deformation, except for macroscopic observations using polycrystalline two-phase alloys and microscopic observation using two-phase composites stacked by very thin films, which are very different from bulk materials. Recently, the two-phase bicrystal of α–β brass was made by Hingwe *et al.* [11, 12] using a specialized heat-treatment technique. They reported some deformation behaviour in the bicrystals. The present authors have also succeeded in making two-phase bicrystals of α–β brass consisting of f c c (α) and b c c (β) single crystals by the diffusion couple method, which is essentially different from Hingwe's method. These two-phase bicrystals are geometrically simple and bulk-like, and in addition it is possible to analyse them precisely and observe their phase-interface structures. Thus, a series of experiments using these bicrystals could be systematically carried out to determine the behaviour of the phase-boundary during plastic deformation.

The purpose of the present study is to analyse the slip traces in each phase activated during yielding, and to clarify the deformation mechanism in connection with the plastic properties of

---

*On leave from Mechanical Engineering Department, Faculty of Engineering, Al-Azhar University, Cairo, Egypt.

each phase, and the interaction between phases and interface structures.

2. Experimental procedure

2.1. Specimen preparation

The chemical compositions of α- and β-brass ingots melted from high purity copper and zinc were 30 and 47.7 wt% Zn respectively. Single crystals of 10 to 20 mm in width, 2 mm in thickness and 100 to 200 mm in length were cut, abrased and then electro-polished in a solution bath of three parts of phosphoric acid, one part of water and one part of ethylalcohol at 273 K. A two-phase bicrystal was made by the "interface migration" method in an α–β diffusion couple; that is, two single crystal plates were placed together in the special graphite holder as shown in Fig. 1. They were then gently fastened with two graphite screws. Since the thermal expansion coefficients are very different for metals and graphite, the coupled specimen is compressed homogeneously when the temperature is raised. Thus the tight bonding of the two alloys promotes diffusion through the interface, without injuring either single crystal. In order to avoid dezincification, the holder was wrapped in copper foil and annealed in an Ar atmosphere. Diffusion annealing treatment was carried out at 873 K for one week. The specimen quenched into iced water immediately after annealing showed a β-layer of about 1 mm thickness grown into the α-phase, although this β-layer occasionally grew in the polycrystalline form.

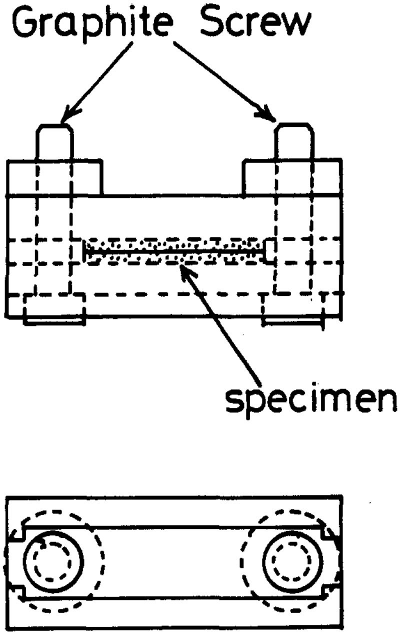

Figure 1 Schematic illustration of the special graphite holder.

Tensile specimens 18 mm in length, 3 mm in width and 2 mm in thickness were cut by a spark-cutting machine, the phase interface being parallel to the tensile axis. Before tensile testing, the specimens were electro-polished in the solution described above.

2.2. Observation procedure

The orientation of each phase was determined by the X-ray Laue method. The concentration profile was measured by an EMX-SM electron probe microanalyser. The concentration–distance relationship in the bicrystals was determined by a point counting technique along a line perpendicular to the α/β interface, using a calibration curve for the relative intensity versus composition.

Tensile tests were carried out at room temperature using an Instron-type machine with a cross-head speed of 0.05 mm min^{-1}. Most specimens were strained up to about 3% plastic strain, but a few specimens were held at strains smaller than

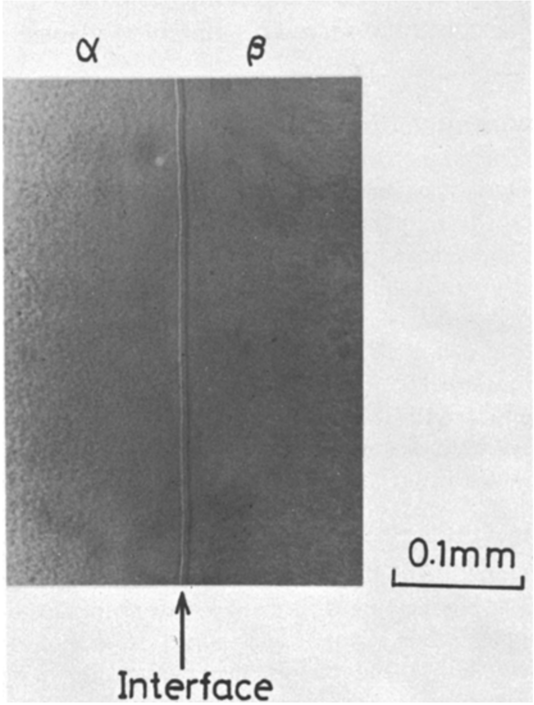

Figure 2 Sharp α–β phase boundary in a two-phase bicrystal. (The left and right regions show the α- and β-phases respectively).

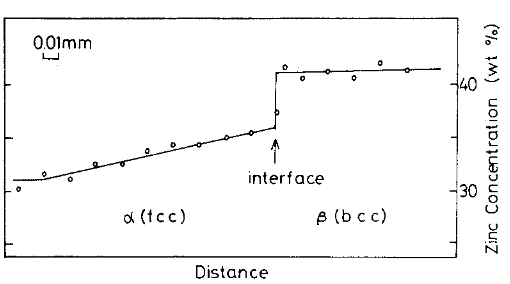

Figure 3 Concentration profile near the interface in a two-phase bicrystal.

this. The slip traces activated within each phase and near the interfaces were observed by optical microscopy and analysed by a two-surface method.

3. Results

3.1. Properties of two-phase bicrystals

A micrograph of a phase boundary is shown in Fig. 2. It can be seen that the phase boundary in the bicrystal obtained by the present technique forms a very flat plane along the whole gauge section. This flatness was not altered, even when the orientation of the original α single crystals was varied. The Zn-concentration profile near the interface as determined by X-ray microanalyser is shown in Fig. 3. The profiles obtained by using a counting method every 16 μm show that the β-region has no concentration gradient but the α-region has a slight gradient of approximately 4 wt % Zn. This concentration difference may induce the change in behaviour depending on "concentration" and the additional change depending on "gradient". The latter effect is caused by the misfit dislocations [13–16]. However, since the properties, in particular the mechanical properties of the α-phase, may not be affected by the slight difference in zinc concentration [17], it is thought that the concentration difference will not invalidate our interpretation of the deformation of α–β brass two-phase bicrystals.

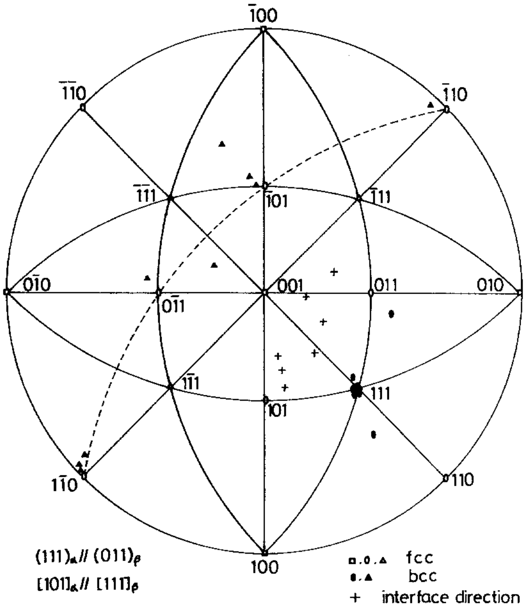

Figure 4 Stereographic projection showing the orientation relationships between the α-and β-phases.

Fig. 4 shows the orientation relationships between the α-and β-phases in the bicrystals made by the present technique. The orientations of some β-phases were plotted on the standard (1 0 0) projection of the α-phase. Unfilled and filled points represent poles of planes for the α-and β-phases respectively. Crosses show the directions normal to the interfaces. It was recongnized that the (1 1 1) planes of the α-phases coincide with the (1 1 0) planes of the β-phases within a few degrees, and the [1 1 0] directions of the α-phases coincide with the [1 1 1] directions of the β-phases with a rather wider scattering. Work has been done on the orientation relationships between the α-and β-phases in the Cu–Zn alloy system. The Kurjumov–Sachs [18] (K–S) relationships ($\{1\,1\,1\}_\alpha \parallel \{1\,1\,0\}_\beta$, $[1\,1\,0]_\alpha \parallel [1\,1\,1]_\beta$) and Nishiyama [19] (N) relationships ($\{1\,1\,1\}_\alpha \parallel \{1\,1\,0\}_\beta$, $[1\,1\,2]_\alpha \parallel [1\,1\,0]_\beta$) were reported for the precipitation of one of these phases from another phase [20, 21], the peritectic formation of β-phases [22] and the phase layer formed by diffusion [23–25]. However, the ideal orientation difference between these two relationships is only 5°16′. To check the adaptation of our results to these two relationships, the distribution frequency was analysed. The result showed that the frequency for the K–S relationship was sharper than that for the N relationship. Therefore it was concluded that the orientation relationship between the α- and β-phases in the present bicrystals satisfied the K–S relationship. The occurrence of the K–S relationship was interpreted as being due to the lowest lattice mismatch, resulting in the lowest interface energy [25].

We can see the preferential orientations for this relationship from the directions of the interfaces which lie around the $(1\,1\,1)_\alpha$ pole. The $\{1\,1\,1\}$ planes of the α-phase and the $\{1\,1\,0\}$ planes of the

β-phase, which have the smallest inclinations to the interfaces, satisfy the K–S relationships. This type of interface structure is in general called a "plane matching" interface, [26] in which a single set of low index atom planes, i.e. $\{1\,1\,1\}_\alpha$ and $\{1\,1\,0\}_\beta$, is continuous and forms a low energy boundary.

3.2. Slip trace observation

In order to observe the deformation character near yielding, the bicrystals were strained to approximately 3% plastic strain. At strains lower than this, no slip lines in the β-phase could be observed. Photographs taken near the interface of some typical two-phase bicrystals are shown in Fig. 5.

The slip traces activated in the α-phase are clear, straight and band-like, while those in the β-phase are fine and wavy ones. Thus we can see a striking contrast between the configurations of slip traces in the α-and β-phases. Furthermore, it was observed that deformation in each phase progressed primarily by a single-slip system, although double-slip planes were observed occasionally in the α-phase. Examples are shown in Figs. 5a to d of the former and in Figs. 5e and f of the latter.

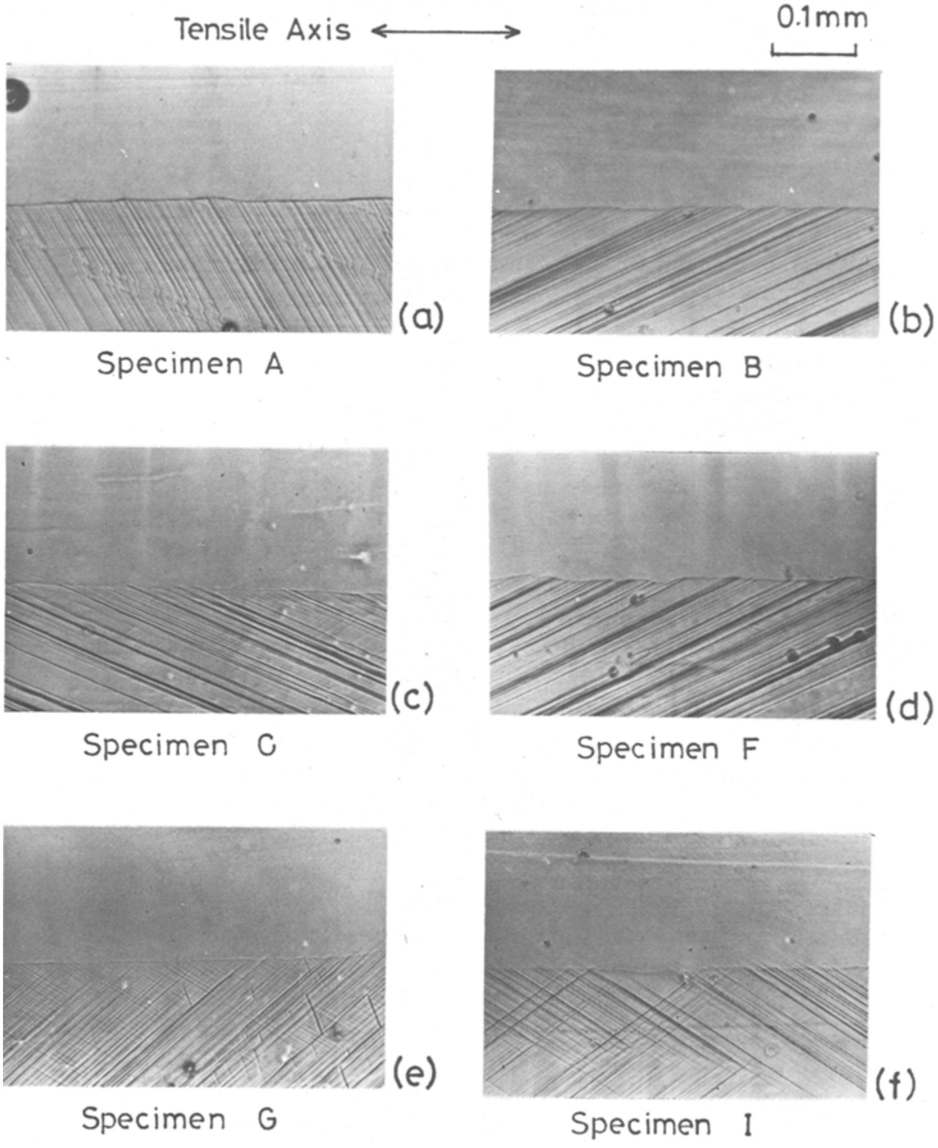

Figure 5 Slip traces activated near interfaces for some two-phase bicrystals. The upper and lower regions show the β-and α-phases respectively. The tensile axis is parallel to the interface.

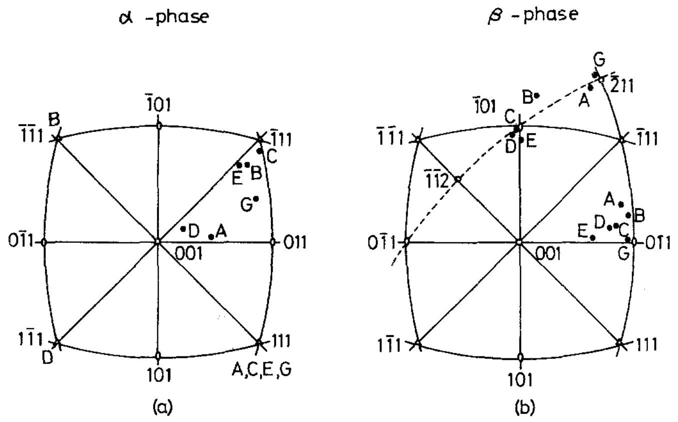

Figure 6 Stereographic projection showing the slip planes activated and the tensile axes the in α-phase (a) and the β-phase (b).

Fig. 6a represents the slip planes activated and the tensile axes in the α-phase, while Fig. 6b represents those in the β-phase. It should be noted that although the primary slip planes were activated in most of the α-phase, the other slip planes which could not be expected from the deformation behaviour of single crystals were observed in a few specimens (for example, specimens B and D). On the other hand, in the β-phase, the $(\bar{1}\,0\,1)$ planes to $(\bar{2}\,1\,1)$ planes along the $\langle 1\,1\,1\rangle$ zone axis were activated although β single crystals are deformed on or near $(\bar{1}\,0\,1)$ planes [27–30]. Thus, slip systems not expected from single crystals were observed, suggesting an interaction between the α- and β-phases.

Slip traces were analysed, noting the "matching planes". Fig. 7a represents the slip trace activated in a bicrystal which has the orientation relationship between the α-and β-phases as shown in Fig. 7b. For this bicrystal, two primary slip planes (i.e. $(1\,1\,1)_\alpha$ and $(\bar{1}\,0\,1)_\beta$) in each phase are coplanar, and two glide directions (i.e. $\langle\bar{1}\,0\,1\rangle_\alpha$ and $\langle 1\,1\,1\rangle_\beta$) in each phase are collinear, and they are continuous at the interface as described in Section

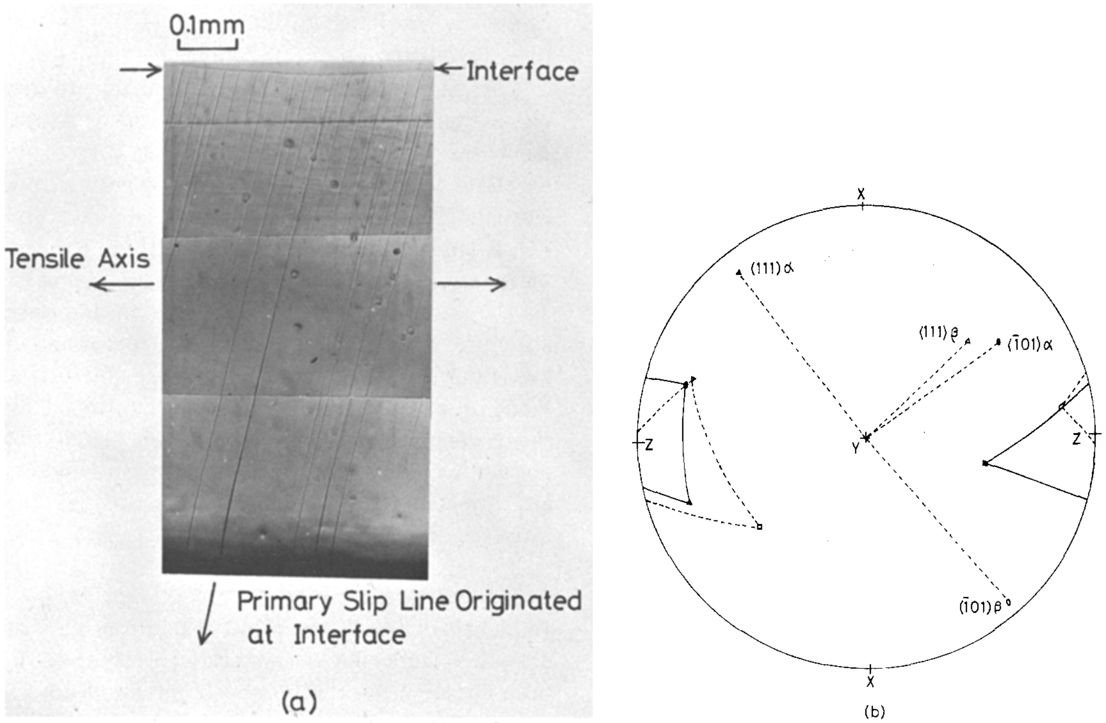

Figure 7 (a) Slip traces activated in the α-phase for a bicrystal which has orientation relationships between the α- and β-phases as shown in Fig. 7b.

3.1. The slip traces given in Fig. 7a are only for the α-phase which was strained to about 0.3% plastic strain, as the slip traces were not observable in the β-phase at this strain. Although slip lines in the α-phase seem to be piled up against the interface, these slip lines are interpreted as originating at the interface or propagating from the β-phase. The reason is as follows: if a slip line originates at an interface or propagates from the β-phase, it should become broader by a double cross-slip mechanism, moving away from the interface. Moreover, from the point of view of continuity of the slip systems at the interface, such behaviour seems to be reasonable. A detailed discussion will be given later.

Slip continuity at an interface between matching planes in each phase can be seen in Fig. 8. The orientation relationship of these two bicrystals shows that the primary slip planes in the α-phases correspond to the matching planes, but in the β-phases do not. The slip traces on the matching planes, in addition to the primary slip traces, are observed in β-phases near interfaces. Consequently, it should be emphasized that the additional slip traces on the matching planes in the β-phase may originate at the interface or propagate from the primary slip traces in the α-phase.

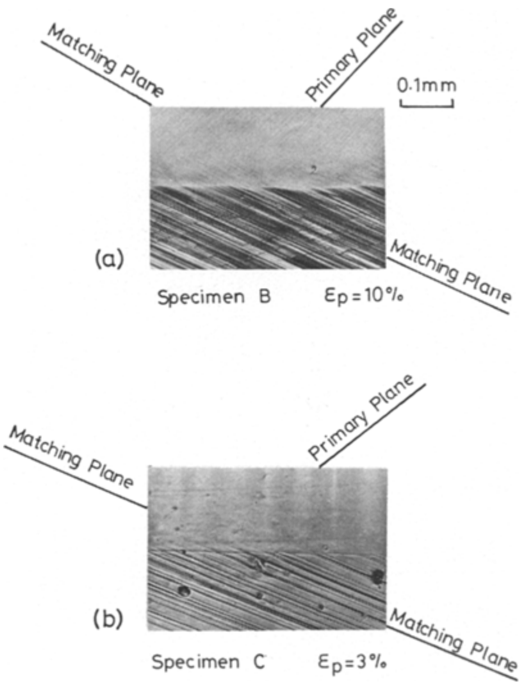

Figure 8 Slip continuity at interface between matching planes in each phases.

4. Discussion

Before discussing the above results, we must consider some fundamental factors controlling the deformation behaviour of α–β brass two-phase bicrystals, both macroscopic and microscopic. We can classify the factors into the following two groups; (1) the properties of respective constituent phases and (2) factors due to the phase-interphase.

The dependence of the deformation behaviour of α-brass single crystals on temperature [17, 31] concentration [17, 31], strain rate [17] and orientation [17, 31, 32] has been reported. The features are consistent with those of other typical fcc structures; the reported slip plane and direction were $\{1\,1\,1\}$ and $[1\,1\,0]$ respectively. On the other hand, the deformation behaviour of β-brass single crystals under various test conditions has also been reported, but was more complicated than that of α single crystals. For instance, slip systems transforming the $\{1\,1\,0\}$ to the $\{1\,1\,2\}$ plane along the $\langle 1\,1\,1\rangle$ zone axis and the $\langle 1\,1\,1\rangle$ direction vary with temperature [27, 28], concentration [29, 30] and deformation mode [29, 33]. In addition, stress-induced martensitic transformations have been reported [34, 35]. Thus it is found that α-brass single crystals deform by the $\{1\,1\,1\}[1\,1\,0]$ slip system, while β single crystals deform by the $\{1\,1\,0\}[1\,1\,1]$ slip system, which can easily be altered to the $\{1\,1\,2\}[1\,1\,1]$ system by a slight variation of test conditions.

Let us now consider the factors due to the phase-interface, both macroscopic and microcopic. As the macroscopic factors we suggest (1) an elastic incompatibility [4, 5] originating from elastic anisotropy between the α- and β-phases and (2) a plastic incompatibility [1, 2] caused by plastic strain mismatch between the α- and β-phases. As the microscopic factor we suggest an interface structure which may control the deformation behaviour of α–β brass two-phase bicrystals. While the macroscopic factors are controlled by the geometrical relationships of each phase with respect to the interface, the microscopic factors are affected by the crystal structure at the interface on an atomic level.

4.1. Macroscopic factors

As shown in Fig. 6, the result that slip planes not expected from single crystals were observed in both phases means that some factors in addition to the applied resolved shear stress must be taken into account. However, the elastic incompatibility factor can be ignored because most bicrystals were strained up to ~3% plastic strain. The incompatibility stress is considered to be a maximum at the interface under elastic strain, but it will be less if the strain increases to plastic strain. Thus this factor is expected to relate to the operation of slip sources at or near boundaries, but is not expected to act effectively at 3% plastic strain.

Consider the plastic strain mismatch at the interface of the two-phase bicrystal on the assumption that one constituent crystal shears on slip system i by a unit distance. If the slip system i is defined by a slip direction g_i and slip plane normal e_i the three strain components of importance at the interface are given as follows;

$$\begin{aligned}\epsilon_{xx} &= (e_i \cdot X)(g_i \cdot X)\\ \epsilon_{zz} &= (e_i \cdot Z)(g_i \cdot Z)\\ \epsilon_{xz} &= \frac{1}{2}[e_i \cdot X)(g_i \cdot Z) + (e_i \cdot Z)(g_i \cdot X)] \quad (1)\end{aligned}$$

where X, Y and Z are unit vectors corresponding to the (x, y, z,) coordinate system of the two-phase bicrystal interface, as shown in Fig. 9. The three important terms of strain mismatch ($\Delta\epsilon_{ij} = |\epsilon_{ij}^{\alpha} - \epsilon_{ij}^{\beta}|$) at the interface were calculated for various combinations of slip systems in α- and β-phases by using Equation 1. The results are given in Table I. In specimen B, the unexpected slip plane was observed in the α-phase, while in specimen A, the unexpected slip plane was observed in the β-phase, as also shown in Fig. 6.

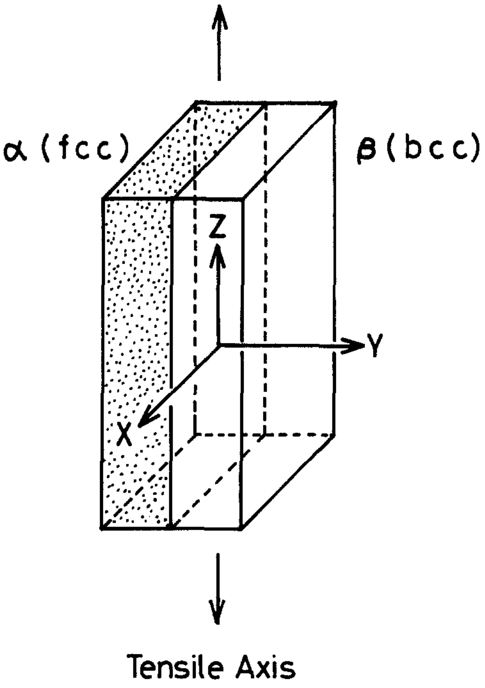

Figure 9 Geometry in a two-phase bicrystal.

In Table I the solid circles on the left indicate the combinations of slip systems which were actually activated, and the solid circles on the right indicate the combinations of slip systems which have the lowest strain mismatch, $\Delta\epsilon_{ij}$. From Table I we note that in both phases the lowest value of strain mismatch is for one of the slip systems among those actually activated. For example, in specimen B it is recognized that

TABLE I Strain mismatch calculated for some combinations of slip systems in the α- and β-phases. The solid circles on the left indicate the combinations of slip systems actually activated and the solid circles on the right indicate the combinations of slip systems which have the lowest values of strain mismatch

Specimen	α ———— β	$\lvert\Delta\epsilon_{xx}\rvert$	$\lvert\Delta\epsilon_{zz}\rvert$	$\lvert\Delta\epsilon_{xz}\rvert$
A	$\bullet\ (1\,1\,1)\langle\bar{1}\,0\,1\rangle$ —•— $P_\beta\langle 1\,1\,1\rangle$	0.026	0.023	0.125
	$(1\,1\,1)\langle\bar{1}\,0\,1\rangle$ ——— $(\bar{1}\,0\,1)\langle 1\,1\,1\rangle$	0.208	0.043	0.279
B	$(1\,1\,1)\langle\bar{1}\,0\,1\rangle$ ——— $(\bar{1}\,0\,1)\langle 1\,1\,1\rangle$	0.018	0.077	0.614
	$(\bar{1}\,\bar{1}\,1)\langle 0\,1\,1\rangle$ —•— $P_\beta\langle 1\,1\,1\rangle$	0.069	0.112	0.119
	$\bullet\ (\bar{1}\,\bar{1}\,1)\langle 1\,0\,1\rangle$ ——— $P_\beta\langle 1\,1\,1\rangle$	0.395	0.170	0.424
	$(\bar{1}\,\bar{1}\,1)\langle 1\,\bar{1}\,0\rangle$ ——— $P_\beta\langle 1\,1\,1\rangle$	0.548	0.492	0.297
C	$\bullet\ (1\,1\,1)\langle\bar{1}\,0\,1\rangle$ —•— $(\bar{1}\,0\,1)\langle 1\,1\,1\rangle$	0.017	0.177	0.018
D	$(1\,1\,1)\langle 1\,0\,1\rangle$ ——— $(\bar{1}\,0\,1)\langle 1\,1\,1\rangle$	0.411	0.771	0.162
	$(1\,\bar{1}\,1)\langle 0\,1\,1\rangle$ ——— $P_\beta\langle 1\,1\,1\rangle$	0.003	0.643	0.754
	$\bullet\ (1\,\bar{1}\,1)\langle\bar{1}\,0\,1\rangle$ ——— $P_\beta\langle 1\,1\,1\rangle$	0.032	0.643	0.363
	$(1\,\bar{1}\,1)\langle 1\,1\,0\rangle$ —•— $P_\beta\langle 1\,1\,1\rangle$	0.021	0.324	0.207
E	$\bullet\ (1\,1\,1)\langle\bar{1}\,0\,1\rangle$ —•— $(\bar{1}\,0\,1)\langle 1\,1\,1\rangle$	0.006	0.056	0.120
F	$\bullet\ (1\,1\,1)\langle\bar{1}\,0\,1\rangle$ —•— $(\bar{1}\,0\,1)\langle 1\,1\,1\rangle$	0.089	0.196	0.056

the strain mismatch for the combination $((1\,1\,1)_\alpha \langle\bar{1}\,0\,1\rangle_\alpha - (\bar{1}\,0\,1)_\beta \langle 1\,1\,1\rangle_\beta)$ of primary slip systems in both phases shows a higher value than that of slip systems actually activated $((\bar{1}\,\bar{1}\,1)_\alpha \langle 0\,1\,1\rangle_\alpha - P_\beta \langle 1\,1\,1\rangle_\beta)$. Here P_β represents the actually determined slip plane with higher index along the $\langle 1\,1\,1\rangle$ zone axis. Also, in specimen A it is seen that the strain mismatch for the combination $((1\,1\,1)_\alpha \langle\bar{1}\,0\,1\rangle_\alpha - (\bar{1}\,0\,1)_\beta \langle 1\,1\,1\rangle_\beta)$ of primary slip systems shows higher values in both phases than that of slip systems actually activated $((1\,1\,1)_\alpha \langle\bar{1}\,0\,1\rangle_\alpha - P_\beta \langle 1\,1\,1\rangle_\beta)$. On the other hand, in specimens which were deformed by primary slip systems in both phases (for instance, specimens C, E and F), the strain mismatch had the lowest values.

It is thought that the slip systems observed in two-phase bicrystals, which are not expected from the deformation behaviour observed in the single crystals, were activated by a "plastic incompatibility" effect. Moreover, we can see that the "plastic incompatibility" effect on the deformation of a two-phase bicrystal is different from the effect on the deformation of a mono-phase bicrystal. In other words, we see that the "plastic incompatibility" effect is characterized by the two-phase bicrystal consisting of f c c and b c c structures, α-brass single crystal cannot deform on any planes other than on $\{1\,1\,1\}$ planes, while the slip plane of β single crystal can be easily changed from the $\{1\,1\,0\}$ plane to the higher index planes along the $\langle 1\,1\,1\rangle$ zone axis by the action of complicated stresses as described above. It is considered that the plastic compatibility effect was responsible for altering the primary $\{1\,1\,1\}$ plane in the α-phase to other $\{1\,1\,1\}$ planes, resulting in a large angle fluctuation, and in the β-phase altering the primary $\{1\,1\,0\}$ to $\{1\,1\,2\}$ planes, resulting in a small angle fluctuation.

4.2. The microscopic factor

This factor can be divided into further two factors; (1) a factor arising from the inequality of the Burgers vector $\boldsymbol{b}$ of dislocations in each phase at the phase-interface, and (2) a factor due to interface dislocations introduced by lattice mismatch.

When a dislocation moves from a glide plane in one phase to a plane in another phase through the interface, the dislocation reacts with other dislocations at the interface. It retains part of the Burgers vectors because the rule of conservation of Burgers vector must be satisfied. The degree of a reaction depends on the magnitude and angle between the Burgers vectors in two phases. It was reported that the Burgers vector of dislocation in α-brass single crystal is the $1/2\ a\ [1\,1\,0]$, while the Burgers vector in β-brass single crystal is the $1/2\ a\ [1\,1\,1]$ [36]. By using the lattice parameters for the chemical compositions in both phases equilibrated at the interface, $a_\alpha = 3.692$ Å and $a_\beta = 2.955$ Å [37], we can obtain the values of the Burgers vectors in both phases i.e. $b_\alpha = 2.611$ Å and $b_\beta = 2.559$ Å. The difference between them is about 2% which is very small. On the other hand, if a dislocation on the matching plane in one phase glides and propagates on another matching plane in another phase through the interface, the angle between the Burgers vectors of dislocations on the two matching planes is very small, as drawn in Fig. 4. Thus, since the matching system $((1\,1\,1)_\alpha \parallel (0\,1\,1)_\beta$ and $[1\,0\,1]_\alpha \parallel [1\,1\,1]_\beta)$, corresponds to the slip system $((1\,1\,1)_\alpha \parallel (0\,1\,1)_\beta$ and $[1\,0\,1]_\alpha \parallel [1\,1\,1]_\beta)$, the dislocations on the matching planes may propagate from one phase to another phase through the interface, or may originate at the interface and then propagate toward the matrices, with little resistance.

Let us now consider the interface dislocations. In order to relax the very small lattice mismatch between $(1\,1\,1)_\alpha$ and $(1\,1\,0)_\beta$ at the interface, the interface dislocations are expected to be intrinsic to the interface. The interface dislocations seem to act as the resistance against the dislocation propagation through the interface. However, the moving dislocation may enter the interface, and then propagate into another phase despite the weak resistance [38, 39]. On the other hand, interface dislocations can act as sources of lattice dislocations [40, 41]. Although some mechanisms for slip nucleation (dislocation nucleation) at interfaces were suggested, we do not intend to discuss detailed mechanisms here.

The α-phase in the bicrystal which was strained to about 0.3% plastic strain, showed slip lines originating at the interface or propagating from the β-phase, as shown in Fig. 7a. When we consider the continuity of slip planes and directions, and the above discussion, we can support this interpretation. Furthermore, in Figs. 8a and b the additional slip traces as well as the primary slip traces were activated on the matching plane in the β-phase. Hence it is emphasized that the additional slip traces limited to near the interface were initiated at the interface or propagated from the α-phases. If we guess these traces to be propagations from the α-phase, the direction of propagation may differ from that observed in Fig. 7a; the slip traces in Fig. 7a seem to propagate from the β-phase, while the slip traces in Figs. 8a and b seem to propagate from the α-phase. Such behaviour could be explained by the sequence of slip deformation in the α-and β-phases, and the preferential propagation toward one phase from the interface which must be controlled by the resolved applied stress, plastic and elastic incompatibility stresses on these planes.

5. Conclusion

In order to clarify the role of phase-interface in deformation of a polycrystalline two-phase alloy, α–β brass two-phase bicrystals consisting of fcc(α) single crystals and bcc(β) single crystals were tensile-tested at room temperature. By observing the slip traces activated during yielding, the following conclusions were drawn:

(1) The two-phase bicrystal made by the solid state diffusion couple method had low concentration gradients in the α- and β-phases, and formed a "plane matching" interface in which the orientation relationships of Kurjumov–Sach's, i.e. $\{1\,1\,1\}_\alpha \parallel \{1\,1\,0\}_\beta$ and $[1\,1\,0]_\alpha \parallel [1\,1\,1]_\beta$ were satisfied.

(2) The slip traces activated in the α-phase appeared to be clear and straight, while the slip traces activated in the β-phase were fine and wavy. Furthermore, the slip systems not expected from the deformation behaviour of single crystals were activated in both phases. The activation of such unexpected slip systems could be interpreted by a "plastic strain incompatibility" mechanism.

(3) The slip systems which seem to originate at interfaces or propagate from another phase were observed on the matching planes.

Acknowledgement

One of the authors (TT) is indebted to the Sakkokai Foundation.

References

1. J. D. LIVINGSTON and B. CHALMERS, *Acta Met.* **5** (1957) 322.
2. J. J. HAUSER and B. CHALMERS, *ibid.* **9** (1961) 802.
3. O. IZUMI and T. TAKASUGI, *Z. Metallkde.* **65** (1974) 542
4. R. E. HOOK and J. P. HIRTH, *Acta Met.* **15** (1967) 535.
5. *Idem, ibid.* **15** (1967) 1099.
6. Y. D. CHAUNG and H. MARGOLIN, *Met. Trans.* **4** (1973) 1905.
7. T. D. LEE and H. MARGOLIN, *Met. Trans. A* **8A** (1977) 145.
8. *Idem ibid.* **8A** (1977) 157.
9. J. D. MOTE and J. E. DORIR, *Trans. AIME* **218** (1960) 491.
10. J. J. GILMAN; *ibid.* **212** (1958) 783.
11. A. K. HINGWE and K. N. SUBRAMANIAN, *J. Crystal Growth* **21** (1974) 287.
12. *Idem, J. Mater. Sci.* **10** (1975) 183.
13. W. R. PATTERSON and I. G. GREENFIELD, *Acta Met.* **19** (1971) 123.
14. Y. G. NAKAGAWA and I. G. GREENFIELD, *ibid.* **21** (1973) 335.
15. *Idem, ibid.* **21** (1973) 367.
16. L. C. D. JONGHE and I. G. GREEFIELD, *ibid.* **17** (1969) 1411.
17. T. E. MITCHEL and P. R. THORNTON, *Phil. Mag.* **8** (1963) 1127.
18. G. KURJUMOV and G. SACHS, *Z. Physik.* **64** (1930) 325.
19. Z. NISHIYAMA, *Sci. Rep. Tohoku Univ.* **23** (1974/5) 637.
20. O. T. MARZKE, *Trans. AIME* **104** (1933) 64.
21. H. HU and C. S. SMITH, *Acta Met.* **4** (1956) 638.
22. A. B. GRENINGER, *Trans. AIME* **124** (1937) 379.
23. S. WOO, C. S. BARRETT and R. F. MEHL, "Metals Technology" (AIME, 1944) p. 1694.
24. K. ITO and H. ABE, *Trans. Japan Inst. Metals.* **14** (1973) 168.
25. M. YAMAMOTO, T. SAKUMA and T. NISHIZAWA, *J. Inst. Japan* **38** (1974) 637.
26. P. H. PUMPHREY, *Scripta Met.* **6** (1972) 107.
27. T. YAMAGATA, H. YOSHIDA and Y. FUKUZAWA, *Trans. Japan Inst. Metals* **17** (1976) 393.
28. S. HANADA, M. MOHRI and O. IZUMI, *ibid.* **16** (1975) 453.
29. M. YAMAGUCHI and Y. UMAKOSHI, *Acta Met.* **24** (1976) 1061.
30. H. M. CLARK, *Phil. Mag.* **15** (1967) 853.
31. P. R. THORNTON and T. E. MITCHELL, *Phil. Mag.* **6** (1961) 361.
32. R. M. MADDIN, C. H. MATHEWSON and W. R. HIBBARD, *Met. Trans.* **185** (1949) 527.
33. A. L. TITCHEUER and W. G. FERGUSON, *J. Inst. Met.* **99** (1971) 345.
34. W. AUNEODO and M. AHLERS, *Acta Met.* **22** (1974) 1475.
35. H. POPS and T. B. MASSALSHI, *Trans. AIME* **230** (1964) 1662.
36. A. E. VIDOZ and L. M. BROWN, *Phil. Mag.* **7** (1962) 1167.
37. L. E. BECK and C. S. SMITH, *J. Metals,* **4** (1952) 1079.
38. T. SCHOBER and R. W. BALLUFFI, *Phil. Mag.* **23** (1971) 165.
39. P. HORTON, J. M. STITCOCK and G. R. KEGG, *Phys. Stat. Sol. (a)* **26** (1974) 215.
40. H. GLEITER, E. HORNBOGEN and G. BÄRO, *Acta Met.* **16** (1968) 1053.
41. J. C. M. LI, *Trans. AIME* **227** (1963) 239.

Received 9 August 1977 and accepted 16 January 1978.